Environmental Pollution 250 (2019) 118–126

Contents lists available at ScienceDirect

Environmental Pollution

journal homepage: www.elsevier.com/locate/envpol

Lead binding to wild metal-resistant bacteria analyzed by ITC and XAFS spectroscopy☆

Hansong Chen [a, b, c], Jinling Xu [a, b], Wenfeng Tan [a], Linchuan Fang [a, d, *]

[a] State Key Laboratory of Soil Erosion and Dryland Farming on the Loess Plateau, Institute of Soil and Water Conservation, Northwest A&F University, Yangling, 712100, China
[b] University of Chinese Academy of Sciences, Beijing, 100049, China
[c] College of Xingzhi, Zhejiang Normal University, Jinhua, 321000, China
[d] CAS Center for Excellence in Quaternary Science and Global Change, Chinese Academy of Sciences, Xian, 710061, China

ARTICLE INFO

Article history:
Received 13 February 2019
Received in revised form
23 March 2019
Accepted 29 March 2019
Available online 9 April 2019

Keywords:
Biosorption
Molecular-scale
Resistant bacteria
Pb
Flagella

ABSTRACT

Metal-resistant bacteria can survive exposure to high metal concentrations without any negative impact on their growth. Biosorption is considered to be one of the more effective detoxification mechanisms acting in most bacteria. However, molecular-scale characterization of metal biosorption by wild metal-resistant bacteria has been limited. In this study, the Pb(II) biosorption behavior of *Serratia* Se1998 isolated from Pb-contaminated soil was investigated through macroscopic and microscopic techniques. A four discrete site non-electrostatic model fit the potentiometric titration data best, suggesting a distribution of phosphodiester, carboxyl, phosphoryl, and amino or hydroxyl groups on the cell surface. The presence of these functional groups was verified by the attenuated total reflection Fourier transform infrared (ATR-FTIR) spectroscopy, which also indicated that carboxyl and phosphoryl sites participated in Pb(II) binding simultaneously. The negative enthalpy ($-9.11\ kJ\ mol^{-1}$) and large positive entropy ($81.52\ J\ mol^{-1}\ K^{-1}$) of Pb(II) binding with the bacteria suggested the formation of inner-sphere complexes by an exothermic process. X-ray absorption fine structure (XAFS) analysis further indicated monodentate inner-sphere binding of Pb(II) through formation of C–O–Pb and P–O–Pb bonds. We inferred that C–O–Pb bonds formed on the flagellar surfaces, establishing a self-protective barrier against exterior metal stressors. This study has important implications for an improved understanding of metal-resistance mechanisms in wild bacteria and provides guidance for the construction of genetically engineered bacteria for remediation purposes.

1. Introduction

The use of microorganisms for immobilization and accumulation of toxic metals has been widely studied as an eco-friendly, cost-effective, and extensively applicable remediation technique (Kang et al., 2014; Chen et al., 2016; Hwang and Jho, 2018). Some bacteria that exhibit resistance to stresses imposed by toxic metal exposure have proved to be ideal tools for bioremediation applications (Kang et al., 2015; Li et al., 2017). Various self-protective strategies have been identified by which these microbes survive exposure to high concentrations of toxic metals without impacts on their growth or metabolism. These include extracellular sequestration, intracellular bioaccumulation, and efflux mechanisms (Naik and Dubey, 2013; Mishra et al., 2017; Wang et al., 2018; Teng et al., 2019). For maintenance of cellular homeostasis, extracellular sequestration serves as the first barrier against entry of toxic metals into microbial cells (Nell et al., 2016). As a particular important interface, the bacterial cell surface and its complex composition play key roles in extracellular sequestration. A better knowledge of how metal binds to the bacterial cell surface at molecular-scale is critical for further characterization of metal-resistance mechanisms, which will consequently provide valuable guidance for practical applications.

Metal ions can be chelated with various functional groups, including carboxyls, phosphoryls, sulfhydryls, hydroxyls, and amino groups, which are ubiquitous to macromolecules on

☆ This paper has been recommended for acceptance by Joerg Rinklebe.

* Corresponding author. State Key Laboratory of Soil Erosion and Dryland Farming on the Loess Plateau, Institute of Soil and Water Conservation, Northwest A&F University, Yangling, 712100, China.
E-mail address: flinc629@hotmail.com (L. Fang).

https://doi.org/10.1016/j.envpol.2019.03.123
0269-7491/

microorganism surfaces, such as lipids, carbohydrates and proteins (Fein et al., 1997; Fang et al., 2010a, 2014; Nell and Fein, 2017). For example, Toner et al. (2005) reported that phosphoryl ligands were key to Zn adsorption on a *Pseudomonas putida* bacterial biofilm, while Guiné et al. (2006) attributed Zn sorption on three Gram-negative bacterial strains predominantly to Zn-sulfhydryl complexes. Using a combination of Fourier transform infrared (FTIR) spectroscopy and X-ray absorption fine structure (XAFS) spectroscopy, Fang et al. (2011) investigated Cu sorption by the cyanobacterium *Spirulina platensis* and demonstrated that Cu-complex formed with two five-membered chelate rings featuring carboxylic ligands. Recently, Qu et al. (2018) reported that Pb ions coordinate with phosphoryl functional groups on *Pseudomonas putida* at low concentrations. These studies demonstrate that the functional groups responsible for metal binding vary among bacterial species and the types of metal they adsorb. However, many previous investigations have focused on common bacteria, especially well-defined strains. Limited information is available regarding the binding mechanisms taking place on cell surfaces of wild metal-resistant bacteria. Recently, Teng et al. (2019) found through X-ray diffraction (XRD) and FTIR spectroscopic analysis that hydroxyl, amide, carboxyl, and phosphate groups were involved in Pb ion binding on the wild Pb-resistant bacterium *Leclercia adecarboxylata*. However, the metal-binding properties of the cell surface were not discussed in further detail.

The involvement of proteins specific to resistant strains may lead to a diversification of active sites on their cell surfaces, making their metal ion binding mechanisms more complex in comparison to common strains. For instance, metal-binding proteins, such as metallothioneins, can sequester and immobilize toxic metals when artificially displayed on the surface of microbial cells, thereby making the metals innocuous (Tafakori et al., 2012). Special metal-binding proteins are also present on the surfaces of wild bacteria. In our recent study, a unique metal-binding flagellin protein with strong metal-binding ability was found in Pb-resistant *Serratia* strains (Chen et al., 2019). We found that one flagellin molecule could bind at least twice as many Pb ions than metallothioneins could, causing the strains to exhibit significantly greater tolerance to Pb. Unlike metallothioneins, flagellin is expressed on the outer surface of bacterial flagella in natural conditions (Braun et al., 2016). How flagellin affects the surface adsorption properties of resistant bacteria is still unclear. Revealing the surface-binding mechanisms on flagella in resistant bacteria is of potential value for bioremediation strategies. Therefore, additional molecular-scale studies are needed to provide insight into the reaction mechanisms on the surfaces of wild metal-resistant bacteria.

In this study, we isolated and identified Pb-resistant strains in contaminated soil collected at a Pb-Zn mine site. A combination of isothermal titration calorimetry (ITC), ATR-FTIR, and XAFS analyses was performed to identify the functional groups and molecular structures that may relate to Pb(II) biosorption on the surface of isolated bacteria. We sought to characterize Pb(II) binding mechanisms at molecular-scale on wild metal-resistant bacteria and to identify unique features by comparing our results with those of previous studies on common strains. We expect these results will shed more light on the mechanisms of toxic metal reactions in wild resistant bacteria and provide guidance for pollution remediation strategies.

2. Materials and methods

2.1. Sampling, isolation, and identification of Pb-resistant bacteria

The strains were isolated from soils surrounding the Pb-Zn mine located in Feng County, Shaanxi province, China (106°35′15″ E, 33°52′35″ N) (Fig. S1). The smelter near the mine has been in operation for over 50 years. A total of 112 samples were collected from 20 sampling sites within 2 km of the mining areas. The soil samples were placed in labeled Ziploc plastic bags for transport to the laboratory and stored at 4 °C after removing weeds and gravel.

To isolate the bacteria from each sample, 10 g of fresh soil was added to a flask containing 90 mL ultrapure water and stirred for 30 min. The large soil particles were then allowed to settle out for 20 min, and 1 mL of supernatant was transferred into 100 mL Bacto™ tryptic soy broth (TSB) containing 2 mM $Pb(NO_3)_2$. After incubation at 28 °C and 180 rpm for 2 days, 0.5 mL of each culture was spread onto a TSB agar plate containing 2 mM $Pb(NO_3)_2$. The plates were then incubated at 28 °C. When colonies were visible on the plates, strains were transferred onto TSB agar plates containing 2–40 mM $Pb(NO_3)_2$. After incubation for another 12 h at 28 °C, a red bacterial colony (Se1998) growing on TSB agar containing 40 mM Pb was isolated and sub-cultured for further assay.

The isolated strain was identified by 16S ribosomal sequence analysis. The highest similarity determined by BLAST analysis (Fig. S2) was to 16S rDNA sequences from the genus *Serratia* (>95%), suggesting it was a *Serratia* strain. *Serratia* is a rod-shaped, Gram-negative flagellate bacterium. Additional details regarding its isolation and identification are described in our previous report (Chen et al., 2019). In all subsequent analyses, this isolate was denoted as *Serratia* Se1998.

2.2. Potentiometric titration

Potentiometric titrations were conducted following the procedure described by Yee et al. (2004) with an automatic titrating instrument (Metrohm 836). Bacterial suspensions (1 g dry weight L^{-1}) were titrated with 0.1059 M HNO_3 and 0.0897 M NaOH solutions under a N_2 atmosphere at 25 °C. Each suspension was initially adjusted to pH ~2.7 with HNO_3 and equilibrated for 30 min, then titrated up to approximately pH 10.0 with NaOH. Before each titration, stabilization to ±0.1 mV s^{-1} was observed. Blank titrations were conducted with 0.01 M KNO_3, which were deducted from the titration curves of the samples.

The acidity constants and concentrations of the functional groups were calculated by a non-electrostatic modeling approach. The deprotonation of a functional group can be represented by the following generic equilibrium (Fein et al., 1997):

$$R - AH^0 \leftrightarrow R - A^- + H^+ \quad (1)$$

where R represents the bacterium to which the functional group, A, is attached. The acidity constant, K_a, for reaction (1) can be expressed as

$$K_\alpha = \frac{[R - A^-]\alpha_{H^+}}{[R - AH^0]} \quad (2)$$

where $[R–A^-]$ and $[R–AH^0]$ are the concentrations of the deprotonated and protonated sites, respectively, and α_{H^+} denotes the activity of protons in the bulk solution.

2.3. Pb(II) adsorption experiments

Batch adsorption experiments were carried out using *Serratia* Se1998 cells at a concentration of 1 g dry weight L^{-1} in 0.01 M KNO_3 background electrolyte. The final Pb(II) concentrations ranged from 0 to 200 mg L^{-1}. The pH of the reaction system was adjusted to 5.5 with 0.1 M HNO_3 and NaOH solutions. According to the Pb chemical speciation calculation by the program ECOSAT (Keizer and Van

Riemsdijk, 1994), no precipitation of Pb occurs at pH 5.5 (Fig. S3). The mixture was shaken at 200 rpm for 4 h at 25 °C. After equilibration, suspensions were centrifuged at 12,000 rpm for 15 min. Following centrifugation, the residual Pb of the supernatant was determined on a Varian 240FS AA spectrometer. The adsorption of Pb(II) was also measured over a range from pH 2.0 to 7.0 in a 1 g L^{-1} bacterial suspension containing 100 mg L^{-1} Pb(II) and 0.01 M KNO_3. A diffuse layer model (DLM) (Borrok, 2005) was adopted to predict the responses of the functional groups to Pb as a function of pH. DLM can be described with the following expression:

$$K_{\text{apparent}} = K_{\text{intrinsic}} \exp\left(\frac{-\Delta z F \psi}{RT}\right) \quad (3)$$

where K_{apparent} (L mol^{-1}) represents the apparent stability constant derived from the non-electrostatic model; $K_{\text{intrinsic}}$ (L mol^{-1}) represents the intrinsic stability constant, which is referenced to conditions of zero surface charge and is unaffected by changes in ionic strength; R (J mol^{-1} K^{-1}) and T (K) are ideal gas constant and absolute temperature, respectively; F (C mol^{-1}) is Faraday constant; Δz denotes the valence change of the surface species; and Ψ (V) is the electric field potential. Ψ can be related to surface charge (σ) using Gouy-Chapman-Stern-Grahame relationship:

$$\psi = (2RT/zF)\sinh^{-1}\left(\frac{\sigma}{\sqrt{8RT\varepsilon_0\varepsilon c}}\right) \quad (4)$$

where z and c (M) refer to the valence and concentration of the counterion, respectively; ε_0 (F m^{-1}) is the vacuum permittivity; and ε (F m^{-1}) is the dielectric constant of water.

2.4. ATR–FTIR spectroscopy

The ATR-FTIR spectra were collected with bacterial cells from the batch experiments performed at various pH values, as well as bacterial cells from solutions containing 100 mg L^{-1} Pb(II) and 0.01 M KNO_3 at pH 5.5. The bacterial cell suspensions were centrifuged at 12,000 rpm for 30 min at 4 °C, and the precipitates were carefully collected. All spectra were recorded in the 600-4000 cm^{-1} at a resolution of 4 cm^{-1} on a Vertex 70 spectrometer (Bruker Optics, Billerica, MA). Prior to measurement of each sample, a 0.01 M KNO_3 solution was used to collect background spectrum at the relevant pH.

2.5. ITC measurement

The measurement of Pb reaction heat on the *Serratia* Se1998 was performed in a TAM III isothermal microcalorimeter (Thermometric AB, Sweden). All titrations were carried out with 0.7 mL of 10 mg dry mass mL^{-1} bacterial cell suspension at 25 °C with stirring at 120 rpm. Titrations were initiated once a stable heat flow with a signal excursion of less than 200 nw h^{-1} was obtained. A total volume of 180 μL Pb(II) solution (0.005 M) was injected into the bacterial cell suspension by a period of 30 min. The titration data, measured as heating flow versus time, was recorded continuously with the TAM assistant software package. To exclude background heat not generated by Pb(II) adsorption, control experiments were conducted by titrating Pb(II) suspension into double-distilled water. Analysis of ITC data was carried out according to the method described in our previous study (Fang et al., 2014). The enthalpy change (ΔH) was derived with the following equation:

$$Q_b = \Delta H\left([M]_T + \frac{(1+nK[L]_T-K[M]_T)-\sqrt{(1+nK[L]_T-K[M]_T)^2+4K[M]_T}}{2K}\right)V_{\text{cell}} \quad (5)$$

where Q_b (kJ) is the total heat of interaction between Pb(II) and the adsorbent; $[L]_T$ (g L^{-1}) and $[M]_T$ (mM) represent the bacterium and metal ion concentrations, respectively; n (mmol g^{-1}) is the total number of binding sites; K (L $mmol^{-1}$) is the equilibrium constant; and V_{cell} (mL) is the volume of sorbent. The change of free energy (ΔG) was obtained by $\Delta G = -RT\ln K$, where R (J mol^{-1} K^{-1}) is the universal gas constant, and T (K) is the absolute temperature. The entropy change (ΔS) was calculated by $\Delta G = \Delta H - T\Delta S$.

2.6. XAFS measurements

Lead L_{III}-edge X-ray absorption spectra at 13,053 eV were collected on the 1W1B beamline at the Beijing Synchrotron Radiation Facility (BSRF). The electron beam energy was 2.5 GeV, with a maximum beam current of 250 mA. The photon flux was above 4×10^{11} ph s^{-1}, and the incident area of the beam on the sample was maintained at 0.9 mm × 0.3 mm. A Pb foil internal reference was used for X-ray energy calibration with the first inflection point set at 13,053 eV. Reference spectra were collected with standard compounds PbO (ortho), 0.1 M $Pb(NO_3)_2$, Pb_3PO_4, and $Pb(OAc)_2 \cdot H_2O$ solutions. The XAFS data from the samples and aqueous complex references were collected in fluorescence mode, while absorption by solid standard compounds was measured in transmittance mode.

Data reduction steps were performed using the IFEFFIT program (Ravel and Newville, 2005). In extracting the $\chi(k)$ function, the XAFS signal was isolated from the absorption edge background by fitting with a cubic spline function. The k^3-weighted $\chi(k)$ function was then Fourier-transformed using the k range 2.5–10.5 $Å^{-1}$ to yield the radial structure function. Data fitting was performed in R space with a multi-shell fitting routine. The FEFF 7.0 code was used to calculate the theoretical scattering phases and amplitudes by input files based on the structural models of PbO, $PbCO_3$ and $Pb_3(PO_4)_2$ (Rehr et al., 1991). The amplitude reduction factor (S_0^2) was fixed at 0.88, based on the fit of the PbO spectral data. The atomic separation distance (R), the coordination number (CN), and the Debye-Waller factor (σ^2) were obtained from the analysis.

3. Results

3.1. Potentiometric titrations

Surface functional groups are the basic units on bacteria to provide potential bind sites for complexation with metal ions (Guiné et al., 2006). In order to determine how many such sites were present on bacterial surfaces in this study, data from each of the titrations were fitted with one, two, three, and four sites using FITEQL (Fig. S4). The corresponding parameters, including acid dissociation constant and site concentrations, are summarized in Table 1. According to the variance between the experimental data and the model, the best fit to the experimental data required a four-site model. The pK_a values for *Serratia* Se1998 were determined to be 4.26, 5.75, 7.82, and 9.68, likely attributable to phosphodiester (pK_a < 4.7), carboxyl (4 < pK_a < 6), phosphoryl (6 < pK_a < 8), and amino (or hydroxy) groups (9 < pK_a < 11), respectively (Fein et al.,

Table 1
FITEQL results for *Serratia* Se1998.

Non-	Bind sites	pK_a[a]	[Site][b]	V(Y)[c]
One site	Does not converge			
Two sites	1	5.57	0.63	43.42
	2	8.93	1.40	
There sites	1	5.07	0.45	7.00
	2	7.22	0.53	
	3	9.47	1.26	
Four sites	1	4.26	0.22	1.11
	2	5.75	0.42	
	3	7.82	0.56	
	4	9.68	1.15	

[a] Average acid dissociation constant, conditional to I = 0.01 M.
[b] Site concentration in 10^{-3} mol g^{-1} normalized to the dry weight of *Serratia* Se1998 cells (1 g L^{-1}, dry wt.).
[c] Variance between the experimental data and the model. A variance of less than 20 suggests a good fit to the experimental data.

1997; Guiné et al., 2006). The corresponding site concentrations were determined to be 0.22×10^{-3}, 0.42×10^{-3}, 0.56×10^{-3}, and 1.15×10^{-3} mol g^{-1} dry weight, respectively.

3.2. Equilibrium adsorption of Pb(II)

The isotherm of Pb(II) adsorption onto *Serratia* Se1998 is shown in Fig. S5, and Table S1 lists the fitting parameters. The large correlation coefficients (R^2) indicated the Langmuir isotherm model fit the data well. The calculated maximum adsorption (Q_m) of Pb(II) to *Serratia* Se1998 was 56.70 mg g^{-1} dry weight, which was significantly greater than that previously reported for some minerals and microbial cells (Sarret et al., 1999; Liang et al., 2017). This suggested that *Serratia* Se1998 has considerable potential for remediation applications.

3.3. pH profile for metal adsorption

Proton concentration (pH) influences the protonation and deprotonation of functional groups which might bind to metal ions. As shown in Fig. 1, the extent of Pb(II) adsorption onto *Serratia* Se1998 increased with pH. One reason for this could have been the generation of negative charges on the bacterial cells by deprotonation (Fang et al., 2011). For a better investigation of the influence of pH on the response of functional groups to Pb, DLM (Borrok, 2005) was adopted to predict the active sites and complexing constants (Table 2). The parameters of DLM are not variable with changes of bacterial surface electric field caused by Pb adsorption, thus minimizing the uncertainty of prediction. The variance between the experimental data we obtained and the model predictions, V(Y), was low, which suggested a good fit between the predictive model output and the corresponding adsorption data input. These results indicated that deprotonation of carboxyl and phosphoryl groups was responsible for increased Pb(II) biosorption at higher pH, likely through formation of a 1:1 complex with Pb(II).

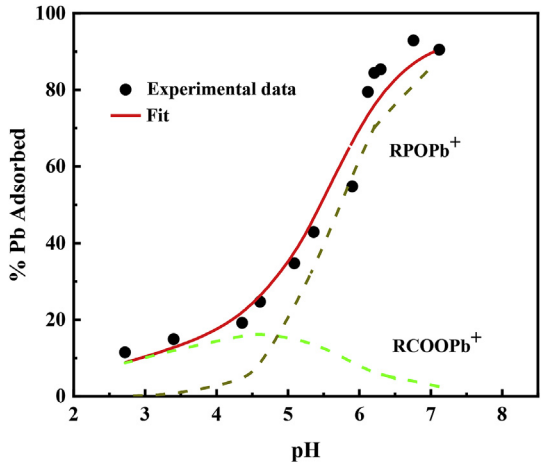

Fig. 1. pH profile for Pb(II) adsorption on the *Serratia* Se1998 in 0.01 M KNO_3 at different pH values.

3.4. ATR-FTIR spectra

Fig. 2 depicts ATR-FTIR spectra for the *Serratia* Se1998 at various pH and exposure to Pb(II). The band assignments are on basis of previous reports (Jiang et al., 2004; Ma et al., 2017). As shown in Fig. 2a, a blue shift in the band at ~1229 cm^{-1}, attributed to −COOH and PO_2^- stretching vibrations, was observed with increasing pH. Moreover, spectra reflecting the various pH conditions revealed a significant increase in peak intensity at ~1404 cm^{-1} (−COO^-) with increasing pH. These phenomena pointed to a contribution from the deprotonation of carboxyl and phosphoryl groups. The result was in agreement with both the DLM predictions at various pH values and band assignments reported by others (Heinrich et al., 2007; Fang et al., 2014).

The exposure of *Serratia* Se1998 to Pb(II) at pH 5.5 led to a significantly different spectrum compared with the untreated bacteria (Fig. 2b). In contrast to the untreated bacteria, the band at ~1057 cm^{-1} (PO_2^-) in the spectra of Pb-exposed cells was apparently not present. The peak intensities at ~1082 cm^{-1} (C−C, C−O−C, and PO_3^{2-} vibrations) and ~1232 cm^{-1} (−COOH and PO_2^- vibrations) were weaker following exposure to Pb(II). The changes observed in the ATR-FTIR spectra suggested that binding of Pb(II) onto *Serratia* Se1998 involved phosphoryl and carboxyl sites.

3.5. Thermodynamic parameters

The power-time curves and cumulative heat of Pb(II) adsorption by *Serratia* Se1998 were adjusted by subtracting the heat of dilution (Fig. 3). Hence, the obtained adsorption heat mainly reflected the thermal effects of sorption between Pb(II) and the bacteria. The thermodynamic parameters are listed in Table 3. The free energy change (ΔG) for the adsorption of Pb by the bacteria was −33.42 kJ mol^{-1}, indicating formation of a stable Pb-bacterium complex via a thermodynamically favorable reaction. The negative ΔH value (−9.11 kJ mol^{-1}) indicated that Pb(II) biosorption was exothermic. In previous reports, adsorption enthalpy varied by both the type of microorganism and the metal that was sorbed, e.g. adsorption of Cu(II) onto *Pseudomonas putida* and *Bacillus thuringiensis* was endothermic (Fang et al., 2010a), while Pb(II) adsorption onto *Pseudomonas putida* was exothermic (Qu et al., 2018). For a wide variety of bacteria, the determined bulk

Table 2
The reaction constants for Pb(II) adsorption on *Serratia* Se1998.

Sample	Complexation reaction	log$K$[a]	V(Y)[b]
Serratia Se1998	$R-COOH + Pb^{2+} = R-COOPb^+ + H^+$	3.16	1.55
	$R-POH + Pb^{2+} = R-POPb^+ + H^+$	3.36	

[a] Complexing constant.
[b] Variance between the experimental data and the model. A variance of less than 20 suggests a good fit to the experimental data.

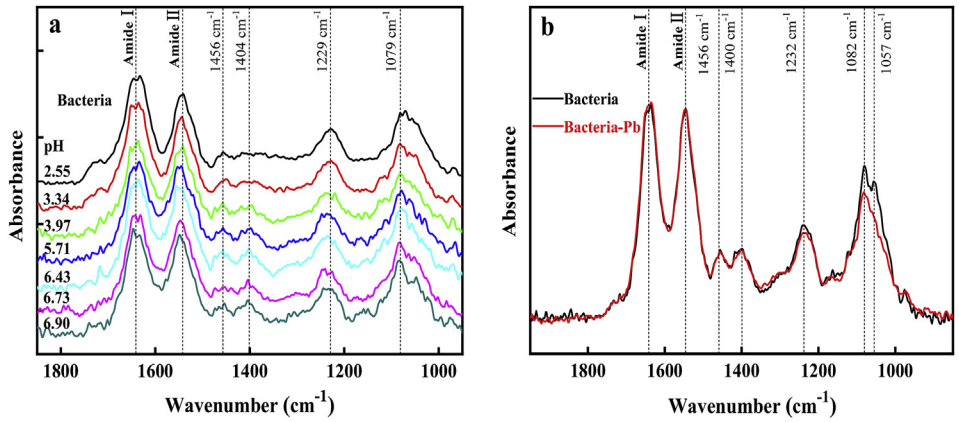

Fig. 2. ATR-FTIR spectra of *Serratia* Se1998 as a function of pH (a) and bacteria exposure to Pb(II) in 0.01 M KNO_3 at pH 5.5 (b) (specified adsorption band shown as dotted lines).

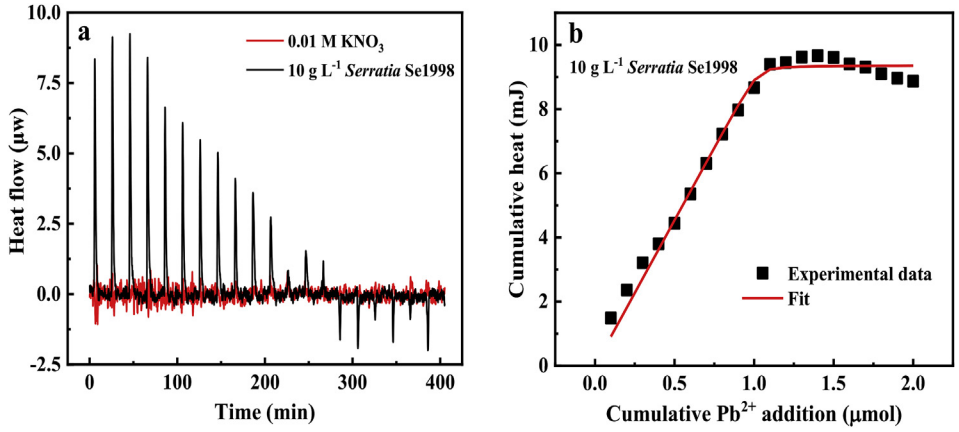

Fig. 3. Power-time curves (a) and cumulative heat (b) for Pb(II) titration into the *Serratia* Se1998 suspension in 0.01 M KNO_3 at pH 5.5 and 25 °C.

Table 3
Thermodynamic parameters for Pb(II) complexation with the *Serratia* Se1998.

Sample	n (mmol g^{-1})	K (L $mmol^{-1}$)	ΔH (kJ mol^{-1})	ΔG (kJ mol^{-1})	ΔS (J mol^{-1} K^{-1})	R^2
Serratia Se1998	0.15	712.63	−9.11	−33.42	81.52	0.992

enthalpies of metal adsorption are all modestly endothermic (Weppen and Hornburg, 1995). Furthermore, complexation entropies can decipher coordination environments of metals and ligands between inner-sphere and outer-sphere complexation. Inner-sphere complexes have positive entropies of complexation, because the complexation displaces solvating water molecules from the coordination sites of the metals and ligands (Gorman-Lewis et al., 2006). The displacement of water molecules causes atomic rearrangement, thereby increasing the randomness of the system, resulting in large positive entropies of complexation (Gorman-Lewis et al., 2006; Du et al., 2016). The observed ΔS of Pb(II) complexation by *Serratia* Se1998 was indisputably positive (81.52 J mol^{-1} K^{-1}), indicating the formation of inner-sphere complexes.

3.6. XAFS analysis

Analyses of X-ray absorption near-edge structure (XANES) and extended X-ray absorption fine structure (EXAFS) are useful to detect oxidation states of ions and their chemical coordination environments in complex systems (Higashi and Takahashi, 2009; Fang et al., 2012; Minkina et al., 2018). Fig. S6 depicts the Pb L_{III}-edge XANES spectra of the samples and reference compounds. The edge positions in samples were similar to those in the Pb(II) model compounds, indicating the oxidation state of lead did not change upon binding to the *Serratia* Se1998 surface. Furthermore, Fig. 4 shows that the EXAFS spectra of samples in both k and R space were similar to those of $Pb_3(PO_4)_2$ and $CH_3COO-Pb^+$, but different from those of $Pb(NO_3)_2$ and PbO (s). The similarities between the spectra of the samples and those of reference compounds containing Pb–phosphoryl and Pb–carboxyl groups suggested the predominant formation of P–O–Pb and C–O–Pb bonds between lead and the *Serratia* Se1998 cells.

The EXAFS spectra were fitted to gain more insight into the molecular structures resulting from Pb(II) binding to *Serratia* Se1998 surfaces. The fitted coordination numbers (CN), atomic separation distances (R), and EXAFS Debye-Waller factors (σ^2) are presented in Table 4. These data suggested that each Pb atom was bound to 2.9 O atoms in the first shell at an average distance of 2.37 Å. In the second coordination shell, the results revealed that Pb(II) was coordinated by 1.0 P atom at a distance of 3.06 Å and 1.0 C atom at a distance of 2.63 Å. Detection of P and C coordinated in the

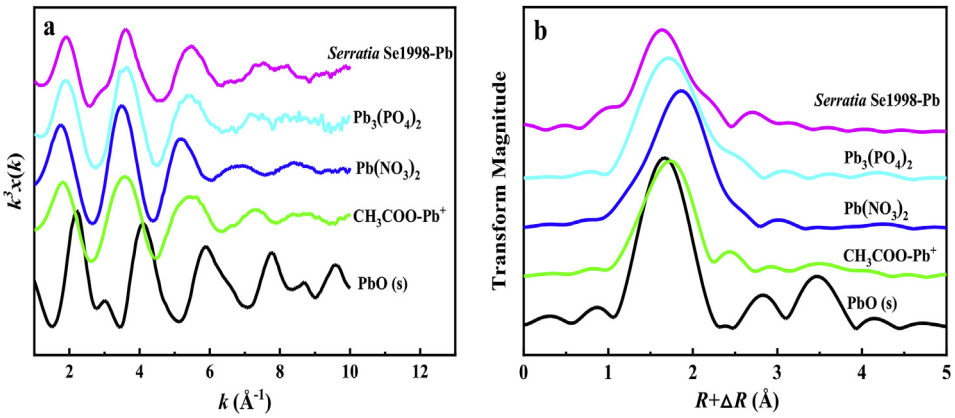

Fig. 4. k^3-weighted EXAFS spectra for Pb of Pb-sorbed bacteria and reference compounds. *k* space (a); *R* space (b).

Table 4
EXAFS fitting results of Pb-sorbed sample and reference compounds.

Sample	Path	CN[a]	*R* (Å)[b]	σ^2 (Å^2)[c]	ΔE_0 (eV)[d]
Serratia Se1998-Pb	Pb–O	2.9	2.37	0.0147	−6.09
	Pb–C	1.0	2.63	0.0020	
	Pb–P	1.0	3.06	0.0447	
$Pb(NO_3)_2$	Pb–O	7.7	2.54	0.0305	−2.90
CH_3COOPb^+	Pb–O	6.5	2.46	0.0256	−2.53
	Pb–C	1.0	2.80	0.0050	
$Pb_3(PO_4)_2$	Pb–O	4.0	2.41	0.0178	−4.99
	Pb–P	2.0	2.94	0.0216	

[a] Coordination number.
[b] Atomic separation distance.
[c] Debye-Waller factor coefficient.
[d] Energy shift.

second shell directly confirmed the inner-sphere complexation of Pb(II) by phosphoryl and carboxyl groups of *Serratia* Se1998. In addition, the coordination numbers of the P and C atoms suggested a monodentate complex structure.

4. Discussion

Biosorption by surface functional groups is considered an important mechanism by which entry of toxic metals into bacterial cells is prevented, which confers resistance to high levels of toxic stress (Naik and Dubey, 2013; Nell and Fein, 2017). Our previous study demonstrated that *Serratia* Se1998 has excellent tolerance for toxic metals (Chen et al., 2019). In the present study, the sorption capacity of *Serratia* Se1998 for Pb(II) was determined to be 56.70 mg g^{-1} dry weight, which is significantly greater than that reported for common strains (12–28 mg g^{-1} dry weight) (Sarret et al., 1999; Qu et al., 2018). These discrepancies could be ascribed to a higher abundance of functional groups on the *Serratia* Se1998 surface. The results of the potentiometric titrations indicate the cell surface of *Serratia* Se1998 contains an abundance of phosphodiester, carboxyl, phosphoryl, and amino (or hydroxyl) groups. The total concentration of functional groups on the surface of *Serratia* Se1998 can reach 2.35×10^{-3} mol g^{-1} dry weight. This is a relatively high value compared to previously reported concentrations among common Gram-negative bacteria (Table 5). This suggests that *Serratia* Se1998 may provide more active sites and thus more potential for immobilizing toxic metals than common strains. These characteristics could be attributed to the complex cell wall framework in the wild strain. *Serratia* Se1998 belongs to a Gram-negative genus, the cell wall of which contains an outer membrane that covers a thin layer of peptidoglycan. The outer membrane is composed of proteins, phospholipids, and lipopolysaccharides. Most of the lipopolysaccharides are concentrated on the outer surface of the membrane, while the phospholipids are concentrated on the inner surface (Ngwenya et al., 2003). Proteins are evenly distributed within the membrane and can be oriented toward either surface (Ngwenya et al., 2003). These cell wall components can provide various functional groups that directly interact with toxic metals, thus preventing the metals from entering the cells (Teng et al., 2019). Further, the pH profiles and results of FTIR spectroscopic analysis obtained in this work revealed that carboxyl and phosphoryl groups contribute most to Pb binding on *Serratia* Se1998. These findings differ slightly from previously reported results obtained with common strains. For example, our previous study (Fang et al., 2011) showed that carboxyl groups are highly efficient in trapping Cu(II) and Cd(II) on the *S. platensis* surface, whereas Qu et al. (2018) reported that Pb(II) adsorption on *P. putida* occurred mainly via phosphoryl groups. These discrepancies could arise from differences among metals and bacterial species, suggesting a single type of functional group tends to govern metal adsorption in common strains. However, our observations with *Serratia* Se1998 imply that synchronous action by various functional groups during biosorption may be a specialty of resistant strains.

The results of our ITC and XAFS analyses further elucidate the mechanisms of interaction between functional groups and toxic metals at the molecular level. The thermodynamic studies establish that Pb(II) forms primarily inner-sphere complexes on *Serratia* Se1998, and that this process is exothermic. Furthermore, the negative value of ΔH (−9.11 kJ mol^{-1}) and positive ΔS (81.52 J mol^{-1} K^{-1}) were observed in this study, which demonstrate that Pb(II) binding to *Serratia* Se1998 is a spontaneous process, and is driven by both entropy and enthalpy (Xu et al., 2018). The XAFS data further provide direct evidence of inner-sphere complexation of Pb(II) through formation of C–O–Pb and P–O–Pb bonds on the *Serratia* Se1998 surface, confirming that carboxyl and phosphoryl groups are the predominant sites of Pb complexation. Inner-sphere complexation with O-containing functional groups has been reported extensively in studies of heavy metal adsorption on common bacterial surfaces, which suggests that metal-bacteria complexes are quite thermodynamically stable (Boyanov et al., 2003; Fang et al., 2010a, b). The C and P coordination numbers in the present work indicate formation of a monodentate complex. Hashimoto et al. (2011) examined the bioavailability of Pb treated

Table 5
Comparison of site concentrations among various Gram-negative bacteria.

Bacteria	pK_a[a]	[Site][b]	Total [Site]	Ref.
Serratia Se1998	4.3	0.22	2.35	This study
	5.8	0.42		
	7.8	0.56		
	9.7	1.15		
G. sulfurreducens	3.2	0.19	0.40	Mishra et al. (2017)
	5.2	0.10		
	7.2	0.04		
	9.5	0.07		
E. coli	2.6	1.29	2.64	Zhao et al. (2015)
	5.7	0.51		
	7.2	0.28		
	9.2	0.56		
P. putida	4.5	0.87	1.85	Wei et al. (2014)
	6.6	0.44		
	9.4	0.54		
Bacterium from Enterobacteriaceae	4.3	0.50	1.27	Ngwenya et al. (2003)
	6.9	0.22		
	8.9	0.55		
S. putrefaciens	5.2	0.03	0.08	Haas et al. (2001)
	7.2	0.01		
	10.0	0.04		

[a] Average acid dissociation constant.
[b] Site concentration in 10^{-3} mol g^{-1} dry weight of bacteria cells.

with organic matter, but they collected less information regarding Pb coordination numbers due to the highly disordered system (Manceau et al., 2002). Liang et al. (2017) reported that Pb(II) was fixed on the surface of magnetite through formation of bidentate binuclear complexes. To our knowledge, this is the first study to directly confirm the monodentate inner-sphere complexation of Pb(II) on wild resistant strains based on calorimetric determinations and analysis of molecular structure. These findings contribute valuable information for enhancing the understanding of metal-microbe interaction mechanisms.

The biosorption of metal ions includes active behavior on the part of functional groups on cell walls and passive behavior involving certain proteins. Proteins specific to resistant bacteria confer more intimate and stable metal-binding properties than are found in common strains. According to previous studies, specific metal-binding proteins, such as metallothioneins (MTs), can sequester and immobilize toxic metals, effectively detoxifying them (Wei et al., 2014; Jafarian and Ghaffari, 2017). We recently found that flagellin played a significant role in Pb binding on *Serratia* Se1998 by exhibiting a higher biosorption capacity than MTs (Chen et al., 2019). Phosphoryl groups are known to have a preferential affinity for Pb compared to carboxyl groups due to formation of P–O–Pb bonds (Gadd and White, 1993; Naik and Dubey, 2013). The results of the present study show that C–O–Pb and P–O–Pb bonds can form simultaneously. Therefore, another reaction interface may be present on which carboxyl groups do not compete with phosphoryl groups. This special interface is likely the bacterial flagellum, as flagellin is a principal constituent of the flagellum. Flagellin is a helical structure with amino acid residues on the outer surface of the folded protein (Braun et al., 2016). These residues mainly include aspartic acid, asparagine, and glutamine containing carboxyl groups (Chen et al., 2019), which facilitate interaction with Pb(II) through formation of C–O–Pb bonds. Hence, the flagellum may not only serve as a locomotive organ, but it may also provide a self-protective barrier against external metal pollutants in metal-resistant bacteria. Strains with abundant flagella are proposed to have more superior toxic metal immobilization and detoxification properties. Furthermore, P–O–Pb bonds could be inferred to form mainly on the cell wall. The lipopolysaccharides and phospholipids of the cell wall are chain molecules linking reactive phosphoryl groups (Kramer et al., 2002; Ngwenya et al., 2003). These components are responsible for the formation of P–O–Pb bonds. The above biosorption behaviors specific to wild resistant strains provide valuable information for strain selection in remediation efforts and for construction of genetically engineered bacteria.

5. Conclusions

Our results demonstrate that *Serratia* Se1998 isolated from Pb-Zn mine soil has high Pb adsorption capacity and good resistance to lead toxicity, which we attribute to a higher concentration of surface functional groups than is found in common stains. Among these functional groups, we confirmed that phosphoryl and carboxyl groups contributed most to binding of Pb(II). Calorimetric determination and coordination environment analysis demonstrated that Pb(II) formed monodentate inner-sphere complexes with these functional groups on the bacterial surface. When combined with the results of our previous work, these findings suggest that flagella contribute to Pb binding by facilitating formation of C–O–Pb bonds. Bacteria with abundant flagella may be ideal microbial species for treatment of toxic metal pollutants, which is valuable information for guidance of remediation strategies.

Acknowledgements

This work was financially supported by the National Natural Science Foundation of China (41571314, 41330852 and 41671406), CAS “Light of West China” Program (XAB2016A03), and Education Department Foundation of Zhejiang Province (Y201738652). We also thank the Beijing Synchrotron Radiation Facility (BSRF, China).

Appendix A. Supplementary data

Supplementary data to this article can be found online at https://doi.org/10.1016/j.envpol.2019.03.123.

References

Borrok, D.M., 2005. Predictive Modeling of Metal Adsorption onto Bacterial Surfaces in Geologic Settings. University of Notre Dame Press, Indiana.

Boyanov, M.I., Kelly, S.D., Kemner, K.M., Bunker, B.A., Fein, J.B., Fowle, D.A., 2003. Adsorption of cadmium to *Bacillus subtilis* bacterial cell walls: a pH-dependent X-ray absorption fine structure spectroscopy study. Geochem. Cosmochim. Acta 67, 3299–3311. https://doi.org/10.1016/s0016-7037(02)01343-1.

Braun, T., Vos, M.R., Kalisman, N., Sherman, N.E., Rachel, R., Wirth, R., Schroeder, G.F., Egelman, E.H., 2016. Archaeal flagellin combines a bacterial type IV pilin domain with an Ig-like domain. Proc. Natl. Acad. Sci. Unit. States Am. 113, 10352–10357. https://doi.org/10.1073/pnas.1607756113.

Chen, B.W., Fang, L.C., Yan, X.T., Zhang, A.Q., Chen, P., Luan, T.G., Hu, L.G., Jiang, G.B., 2019. A unique Pb-binding flagellin as an effective remediation tool for Pb contamination in aquatic environment. J. Hazard Mater. 363, 34–40. https://doi.org/10.1016/j.jhazmat.2018.10.004.

Chen, L., He, L.Y., Wang, Q., Sheng, X.F., 2016. Synergistic effects of plant growth-promoting *Neorhizobium huautlense* T1-17 and immobilizers on the growth and heavy metal accumulation of edible tissues of hot pepper. J. Hazard Mater. 312, 123–131. https://doi.org/10.1016/j.jhazmat.2016.03.042.

Du, H.H., Chen, W.L., Cai, P., Rong, X.M., Feng, X.H., Huang, Q.Y., 2016. Competitive adsorption of Pb and Cd on bacteria-montmorillonite composite. Environ. Pollut. 218, 168–175. https://doi.org/10.1016/j.envpol.2016.08.022.

Fang, L.C., Cai, P., Li, P.X., Wu, H.Y., Liang, W., Rong, X.M., Chen, W.L., Huang, Q.Y., 2010a. Microcalorimetric and potentiometric titration studies on the adsorption of copper by *P. putida* and *B. thuringiensis* and their composites with minerals. J. Hazard Mater. 181, 1031–1038. https://doi.org/10.1016/j.jhazmat.2010.05.118.

Fang, L.C., Cao, Y.Y., Huang, Q.Y., Walker, S.L., Cai, P., 2012. Reactions between bacterial exopolymers and goethite: a combined macroscopic and spectroscopic investigation. Water Res. 46, 5613–5620. https://doi.org/10.1016/j.watres.2012.07.046.

Fang, L.C., Huang, Q.Y., Wei, X., Liang, W., Rong, X.M., Chen, W.L., Cai, P., 2010b. Microcalorimetric and potentiometric titration studies on the adsorption of copper by extracellular polymeric substances (EPS), minerals and their composites. Bioresour. Technol. 101, 5774–5779. https://doi.org/10.1016/j.biortech.2010.02.075.

Fang, L.C., Yang, S.S., Huang, Q.Y., Xue, A.F., Cai, P., 2014. Biosorption mechanisms of Cu(II) by extracellular polymeric substances from *Bacillus subtilis*. Chem. Geol. 386, 143–151. https://doi.org/10.1016/j.chemgeo.2014.08.017.

Fang, L.C., Zhou, C., Cai, P., Chen, W.L., Rong, X.M., Dai, K., Liang, W., Gu, J.D., Huang, Q.Y., 2011. Binding characteristics of copper and cadmium by cyanobacterium *Spirulina platensis*. J. Hazard Mater. 190, 810–815. https://doi.org/10.1016/j.jhazmat.2011.03.122.

Fein, J.B., Daughney, C.J., Yee, N., Davis, T.A., 1997. A chemical equilibrium model for metal adsorption onto bacterial surfaces. Geochem. Cosmochim. Acta 61, 3319–3328. https://doi.org/10.1016/S0016-7037(97)00166-X.

Gadd, G.M., White, C., 1993. Microbial treatment of metal pollution-a working biotechnology. Trends Biotechnol. 11, 353–359. https://doi.org/10.1016/0167-7799(93)90158-6.

Gorman-Lewis, D., Fein, J.B., Jensen, M.P., 2006. Enthalpies and entropies of proton and cadmium adsorption onto *Bacillus subtilis* bacterial cells from calorimetric measurements. Geochem. Cosmochim. Acta 70, 4862–4873. https://doi.org/10.1016/j.gca.2006.07.022.

Guiné, V., Spadini, L., Sarret, G., Muris, M., Delolme, C., Gaudet, J.P., Martins, J.M.F., 2006. Zinc sorption to three gram-negative bacteria: combined titration, modeling, and EXAFS study. Environ. Sci. Technol. 40, 1806–1813. https://doi.org/10.1021/rd050981l.

Haas, J.R., Dichristina, T.J., Wade, R., 2001. Thermodynamics of U(VI) sorption onto *Shewanella putrefaciens*. Chem. Geol. 180, 33–54. https://doi.org/10.1016/s0009-2541(01)00304-7.

Hashimoto, Y., Yamaguchi, N., Takaoka, M., Shiota, K., 2011. EXAFS speciation and phytoavailability of Pb in a contaminated soil amended with compost and gypsum. Sci. Total Environ. 409, 1001–1007. https://doi.org/10.1016/j.scitotenv.2010.11.018.

Heinrich, H.T.M., Bremer, P.J., Daughney, C.J., McQuillan, A.J., 2007. Acid-base titrations of functional groups on the surface of the thermophilic bacterium *Anoxybacillus flavithermus*: comparing a chemical equilibrium model with ATR-IR spectroscopic data. Langmuir 23, 2731–2740. https://doi.org/10.1021/la062401j.

Higashi, M., Takahashi, Y., 2009. Detection of S(IV) species in aerosol particles using XANES spectroscopy. Environ. Sci. Technol. 43, 7357–7363. https://doi.org/10.1021/es900163y.

Hwang, S.Y., Jho, E.H., 2018. Heavy metal and sulfate removal from sulfate-rich synthetic mine drainages using sulfate reducing bacteria. Sci. Total Environ. 635, 1308–1316. https://doi.org/10.1016/j.scitotenv.2018.04.231.

Jafarian, V., Ghaffari, F., 2017. A unique metallothionein-engineered in *Escherichia coli* for biosorption of lead, zinc, and cadmium; absorption or adsorption? Microbiology 86, 73–81. https://doi.org/10.1134/s0026261717010064.

Jiang, W., Saxena, A., Song, B., Ward, B.B., Beveridge, T.J., Myneni, S.C.B., 2004. Elucidation of functional groups on gram-positive and gram-negative bacterial surfaces using infrared spectroscopy. Langmuir 20, 11433–11442. https://doi.org/10.1021/la049043+.

Kang, C.H., Choi, J.H., Noh, J.G., Kwak, D.Y., Han, S.H., So, J.S., 2014. Microbially induced calcite precipitation-based sequestration of strontium by *Sporosarcina pasteurii* WJ-2. Appl. Biochem. Biotechnol. 174, 2482–2491. https://doi.org/10.1007/s12010-014-1196-4.

Kang, C.H., Oh, S.J., Shin, Y., Han, S.H., Nam, I.H., So, J.S., 2015. Bioremediation of lead by ureolytic bacteria isolated from soil at abandoned metal mines in South Korea. Ecol. Eng. 74, 402–407. https://doi.org/10.1016/j.ecoleng.2014.10.009.

Keizer, M., Van Riemsdijk, W., 1994. ECOSAT: Equilibrium Calculation of Speciation and Transport. Manual Program Agricultural University Press, Wageningen.

Kramer, R.A., Brandenburg, K., Vandeputte-Rutten, L., Werkhoven, M., Gros, P., Dekker, N., Egmond, M., 2002. Lipopolysaccharide regions involved in the activation of Escherichia coli outer membrane protease OmpT. Eur. J. Biochem. 269, 1746–1752. https://doi.org/10.1046/j.1432-1327.2002.02820.x.

Li, Y., Pang, H.D., He, L.Y., Wang, Q., Sheng, X.F., 2017. Cd immobilization and reduced tissue Cd accumulation of rice (*Oryza sativa* wuyun-23) in the presence of heavy metal-resistant bacteria. Ecotoxicol. Environ. Saf. 138, 56–63. https://doi.org/10.1016/j.ecoenv.2016.12.024.

Liang, X.L., Wei, G.L., Xiong, J., Tan, F.D., He, H.P., Qu, C.C., Yin, H., Zhu, J.X., Zhu, R.L., Qin, Z.H., Zhang, J., 2017. Adsorption isotherm, mechanism, and geometry of Pb(II) on magnetites substituted with transition metals. Chem. Geol. 470, 132–140. https://doi.org/10.1016/j.chemgeo.2017.09.003.

Ma, W.T., Peng, D.H., Walker, S.L., Cao, B., Gao, C.H., Huang, Q.Y., Cai, P., 2017. *Bacillus subtilis* biofilm development in the presence of soil clay minerals and iron oxides. Npj Biofilms Microbi. 3, 1–9. https://doi.org/10.1038/s41522-017-0013-6.

Manceau, A., Lanson, B., Drits, V.A., 2002. Structure of heavy metal sorbed birnessite. Part III: results from powder and polarized extended X-ray absorption fine structure spectroscopy. Geochem. Cosmochim. Acta 66, 2639–2663. https://doi.org/10.1016/s0016-7037(02)00869-4.

Minkina, T., Nevidomskaya, D., Bauer, T., Shuvaeva, V., Soldatov, A., Mandzhieva, S., Zubavichus, Y., Trigub, A., 2018. Determining the speciation of Zn in soils around the sediment ponds of chemical plants by XRD and XAFS spectroscopy and sequential extraction. Sci. Total Environ. 634, 1165–1173. https://doi.org/10.1016/j.scitotenv.2018.04.118.

Mishra, B., Shoenfelt, E., Yu, Q., Yee, N., Fein, J.B., Myneni, S.C.B., 2017. Stoichiometry of mercury-thiol complexes on bacterial cell envelopes. Chem. Geol. 464, 137–146. https://doi.org/10.1016/j.chemgeo.2017.02.015.

Naik, M.M., Dubey, S.K., 2013. Lead resistant bacteria: lead resistance mechanisms, their applications in lead bioremediation and biomonitoring. Ecotoxicol. Environ. Saf. 98, 1–7. https://doi.org/10.1016/j.ecoenv.2013.09.039.

Nell, R.M., Fein, J.B., 2017. Influence of sulfhydryl sites on metal binding by bacteria. Geochem. Cosmochim. Acta 199, 210–221. https://doi.org/10.1016/j.gca.2016.11.039.

Nell, R.M., Szymanowski, J.E.S., Fein, J.B., 2016. Divalent metal cation adsorption onto *Leptothrix cholodnii* SP-6SL bacterial cells. Chem. Geol. 439, 132–138. https://doi.org/10.1016/j.chemgeo.2016.06.021.

Ngwenya, B.T., Sutherland, I.W., Kennedy, L., 2003. Comparison of the acid-base behaviour and metal adsorption characteristics of a gram-negative bacterium with other strains. Appl. Geochem. 18, 527–538. https://doi.org/10.1016/s0883-2927(02)00118-x.

Qu, C.C., Du, H.H., Ma, M.K., Chen, W.L., Cai, P., Huang, Q.Y., 2018. Pb sorption on montmorillonite-bacteria composites: a combination study by XAFS, ITC and SCM. Chemosphere 200, 427–436. https://doi.org/10.1016/j.chemosphere.2018.02.136.

Ravel, B., Newville, M., 2005. ATHENA, ARTEMIS, HEPHAESTUS: data analysis for X-ray absorption spectroscopy using IFEFFIT. J. Synchrotron Radiat. 12, 537–541. https://doi.org/10.1107/s0909049505012719.

Rehr, J.J., Mustre de Leon, J., Zabinsky, S.I., Albers, R.C., 1991. Theoretical X-ray absorption fine structure standards. J. Am. Chem. Soc. 113, 5135–5140. https://doi.org/10.1021/ja00014a001.

Sarret, G., Manceau, A., Spadini, L., Roux, J.C., Hazemann, J.L., Soldo, Y., Eybert-Berard, L., Menthonnex, J.J., 1999. Structural determination of Pb binding sites in *Penicillium chrysogenum* cell walls by EXAFS spectroscopy and solution chemistry. J. Synchrotron Radiat. 6, 414–416. https://doi.org/10.1107/s0909049598014162.

Tafakori, V., Ahmadian, G., Amoozegar, M.A., 2012. Surface display of bacterial metallothioneins and a chitin binding domain on *Escherichia coli* increase cadmium adsorption and cell immobilization. Appl. Biochem. Biotechnol. 167, 462–473. https://doi.org/10.1007/s12010-012-9684-x.

Teng, Z., Shao, W., Zhang, K., Huo, Y., Li, M., 2019. Characterization of phosphate solubilizing bacteria isolated from heavy metal contaminated soils and their potential for lead immobilization. J. Environ. Manag. 231, 189–197. https://doi.org/10.1016/j.jenvman.2018.10.012.

Toner, B., Manceau, A., Marcus, M.A., Millet, D.B., Sposito, G., 2005. Zinc sorption by a bacterial biofilm. Environ. Sci. Technol. 39, 8288–8294. https://doi.org/10.1021/es050528+.

Wang, X.H., Luo, W.W., Wang, Q., He, L.Y., Sheng, X.F., 2018. Metal(loid)-resistant bacteria reduce wheat Cd and as uptake in metal(loid)-contaminated soil. Environ. Pollut. 241, 529–539. https://doi.org/10.1016/j.envpol.2018.05.088.

Wei, W., Liu, X.Z., Sun, P.Q., Wang, X., Zhu, H., Hong, M., Mao, Z.W., Zhao, J., 2014. Simple whole-cell biodetection and bioremediation of heavy metals based on an engineered lead-specific operon. Environ. Sci. Technol. 48, 3363–3371.

https://doi.org/10.1021/es4046567.
Weppen, P., Hornburg, A., 1995. Calorimetric studies on interactions of divalent cations and microorganisms or microbial envelopes. Thermochim. Acta 269, 393–404. https://doi.org/10.1016/0040-6031(95)02515-4.
Xu, J.L., Koopal, L.K., Fang, L.C., Xiong, J., Tan, W.F., 2018. Proton and copper binding to humic acids analyzed by XAFS spectroscopy and isothermal titration calorimetry. Environ. Sci. Technol. 52, 4099–4107. https://doi.org/10.1021/acs.est.7b06281.
Yee, N., Benning, L.G., Phoenix, V.R., Ferris, F.G., 2004. Characterization of metal-cyanobacteria sorption reactions: a combined macroscopic and infrared spectroscopic investigation. Environ. Sci. Technol. 38, 775–782. https://doi.org/10.1021/es0346680.
Zhao, W.Q., Yang, S.S., Huang, Q., Cai, P., 2015. Bacterial cell surface properties: role of loosely bound extracellular polymeric substances (LB-EPS). Colloids Surf., B 128, 600–607. https://doi.org/10.1016/j.colsurfb.2015.03.017.